bioRxiv preprint doi: https://doi.org/10.1101/337402; this version posted June 2, 2018. The copyright holder for this preprint (which was not certified by peer review) is the author/funder. All rights reserved. No reuse allowed without permission.

1 **Enhanced Synthesis of Poly Gamma Glutamic Acid by Increasing the**
2 **Intracellular Reactive Oxygen Species in the *Bacillus licheniformis***
3 **Δ1-pyrroline-5-carboxylate Dehydrogenase Gene *ycgN* Deficient Strain**

4 **Running title: Deletion of *ycgN* Enhanced γ-PGA Synthesis**

5 **Bichan Li,** [a, b] **Dongbo Cai,** [c] **Shiying Hu,** [c] **Anting Zhu,** [c] **Zhili He,** [a, d] **Shouwen Chen** [a, c]

6 [a] *State Key Laboratory of Agricultural Microbiology, College of Life Science and*
7 *Technology, Huazhong Agricultural University, Wuhan 430070, People's Republic of*
8 *China*

9 [b] *Fujian Provincial Key Laboratory of Eco-Industrial Green Technology, College of*
10 *Ecological and Resource Engineering, Wuyi University, Wuyishan 354300, People's*
11 *Republic of China*

12 [c] *Environmental Microbial Technology Center of Hubei Province, Hubei Collaborative*
13 *Innovation Center for Green Transformation of Bio-Resources, College of Life Sciences,*
14 *Hubei University, Wuhan 430062, People's Republic of China*

15 [d] *Environmental Microbiomics Research Center, School of Environmental Science and*
16 *Engineering, Sun Yat-Sen University, Guangzhou 510006, People's Republic of China*

17 *Corresponding author. Shouwen Chen

18 Tel./fax.: +86 027-87280670.

19 *E-mail address*: mel212@126.com (S. Chen).

20 *Postal address*: No. 368 Youyi Avenue, Wuchang District, Wuhan 430062, Hubei, PR
21 China

22

bioRxiv preprint doi: https://doi.org/10.1101/337402; this version posted June 2, 2018. The copyright holder for this preprint (which was not certified by peer review) is the author/funder. All rights reserved. No reuse allowed without permission.

23 **Abstract** Poly gamma glutamic acid (γ-PGA) is an anionic polyamide with numerous applications. Proline
24 metabolism influences the formation of reactive oxygen species (ROS), and is involved in a wide range of
25 cellular processes. However, the relation between proline metabolism and γ-PGA synthesis has not yet been
26 analyzed. In this study, our results indicated that the deletion of Δ1-pyrroline-5-carboxylate dehydrogenase
27 encoded gene *ycgN* resulted in 85.22% higher yield of γ-PGA in *B. licheniformis* WX-02. But the deletion
28 of proline dehydrogenase encoded gene *ycgM* had no effect on γ-PGA synthesis. Meanwhile, a 2.92-fold
29 higher level of P5C was detected in *ycgN* deficient strain WXΔ*ycgN*, while the P5C levels in WXΔ*ycgM*
30 and double mutant strain WXΔ*ycgMN* remained the same, compared to WX-02. The ROS level of
31 WXΔ*ycgN* was 1.18-fold higher than that of WX-02, and the addition of n-acetylcysteine (antioxidant) into
32 medium could decrease its ROS level, further reduced the γ-PGA yield. Our results showed that proline
33 catabolism played an important role in maintaining ROS homeostasis, and the deletion of *ycgN* caused P5C
34 accumulation, which induced a transient ROS signal to promote γ-PGA synthesis in *B. licheniformis*.

35

36 **Importance** γ-PGA is an anionic polyamide with various applications in biomedical and industrial fields.
37 Proline metabolism influences the intracellular reactive oxygen species (ROS) and is involved in a wide
38 range of cellular processes. Here, we report the effects of proline metabolism on γ-PGA synthesis. Our
39 results indicated that deletion of *ycgN* promoted the synthesis of γ-PGA by increasing the intracellular
40 levels of Δ1-pyrroline-5-carboxylate to generate a transient ROS signal in *B. licheniformis* WX-02. This
41 study provides the valuable information that enhanced synthesis of γ-PGA by knocking out of *ycgN*.

42

43 **Keywords: Poly gamma glutamic acid, Proline metabolism, YcgN, Reactive oxygen species, *Bacillus***

bioRxiv preprint doi: https://doi.org/10.1101/337402; this version posted June 2, 2018. The copyright holder for this preprint (which was not certified by peer review) is the author/funder. All rights reserved. No reuse allowed without permission.

44 ***licheniformis***

45

46

bioRxiv preprint doi: https://doi.org/10.1101/337402; this version posted June 2, 2018. The copyright holder for this preprint (which was not certified by peer review) is the author/funder. All rights reserved. No reuse allowed without permission.

47 **Introduction**

48 Poly gamma glutamic acid (γ-PGA) is an anionic polyamide which consists of D- and L-glutamic acid
49 units connected by γ-amide linkages between γ-carboxyl and α-amino groups (1-3). With its features of
50 hygroscopicity, water-solubility, biodegradability, non-toxicity and cation chelating, γ-PGA has been widely
51 used in the fields of medicine, food, cosmetics, agriculture, water treatment, etc. (4). For example, γ-PGA
52 can be served as the drug carrier in medicine, thickener and cryoprotectant in food industry, humectant in
53 cosmetics, fertilizer synergist in agriculture, flocculants and heavy metal absorbent in water treatment (1, 4,
54 5) .

55 γ-PGA is mainly produced by *Bacillus* species as an extracellular polymer (4, 6-8). Several strategies
56 have been conducted to improve γ-PGA production via metabolic engineering of γ-PGA synthesis-related
57 metabolic network (9). For instance, γ-PGA yield was enhanced by 63.2% in *B. amyloliquefaciens* LL3 via
58 double-deletion of genes *cwlO* (encodes a cell wall lytic enzyme) and *epsA-O* cluster (responsible for
59 extracellular polysaccharide synthesis), as well as introduction of the gene *vgb* (encodes *Vitreoscilla*
60 hemoglobin) (10). Another example is that a systematically metabolic engineering study consisting the
61 by-products synthesis, γ-PGA degradation, glutamate precursor synthesis, γ-PGA synthesis and autoinducer
62 synthesis pathways has been performed in *B. amyloliquefaciens* NK-1, and the γ-PGA yield was increased
63 by 2.91-fold in the final strain NK-anti-*rocG* (11). In our previous work, over-expression of *glr* (encodes
64 glutamic acid racemase) (12), *pgdS* (encodes γ-PGA hydrolase) (3), *zwf* gene (encodes glucose-6-phosphate
65 dehydrogenase) (13), *rocG* (encodes glutamate dehydrogenase) (14), and *fnr* (encodes global anaerobic
66 regulator) (15) could all enhance γ-PGA production in *B. licheniformis* WX-02. Also, improving the
67 capability of assimilating glycerol was proved to be an efficient strategy to increase γ-PGA yield, and the

bioRxiv preprint doi: https://doi.org/10.1101/337402; this version posted June 2, 2018. The copyright holder for this preprint (which was not certified by peer review) is the author/funder. All rights reserved. No reuse allowed without permission.

68 γ-PGA concentration was improved by 33.71% by substituting the native *glpFK* promoter with the
69 constitutive promoter P43 (16).

70 Proline is a multifaceted amino acid with important roles in carbon and nitrogen metabolism, protein
71 synthesis, bioenergetics, differentiation, growth, etc. (17-19). Proline is oxidated to glutamate by proline
72 dehydrogenase (PRODH) and Δ1-pyrroline-5-carboxylate dehydrogenase (P5CDH), involved a
73 four-electron oxidation process (**Fig. 1**) (18). Firstly, proline is oxidized to Δ1-pyrroline-5-carboxylate (P5C)
74 by O_2-dependent PRODH, which is non-enzymatically transformed into glutamate-γ-semialdehyde (GSA),
75 and then oxidized to glutamate by P5CDH (18, 20). Recent studies demonstrated that proline metabolism
76 plays an important role in maintaining the balance of intracellular reactive oxygen species (ROS), and
77 influenced numerous additional regulatory pathways, such as p53-mediated apoptosis in mammalian cells
78 (21) and osmo-protecting mechanisms in plants(17) and bacteria(18, 22), etc. There are two possible
79 mechanisms for the ROS generation. First, ROS is supposed to be generated from P5C-proline cycle, which
80 is catalyzed by PRODH and P5C reductase (**Fig1**) (17, 23, 24). The P5C-proline cycle provides an excess
81 of electron flow to the electron transport chain (ETC) and O_2 which further induces ROS overproduction
82 (17, 23, 24). Second, ROS is spontaneously generated from the intermediate of proline metabolism
83 P5C/GSA, which has the high activity with various cellular compounds (25, 26). In budding yeast, P5C
84 directly inhibits the mitochondrial respiration and induces a burst of superoxide anions from the
85 mitochondria (24). Since addition of H_2O_2 was proven as an efficient strategy for enhancement of γ-PGA
86 yield by improving the intracellular ROS (9), we hypothesized that the manipulating of proline metabolism
87 might also affect γ-PGA synthesis.

88 Reactive oxygen species (ROS), such as superoxide ($O_2^-\cdot$), hydrogen peroxide (H_2O_2), and hydroxyl

bioRxiv preprint doi: https://doi.org/10.1101/337402; this version posted June 2, 2018. The copyright holder for this preprint (which was not certified by peer review) is the author/funder. All rights reserved. No reuse allowed without permission.

89 radical (OH·), are highly reactive molecules. They mediate a number of significant cell processes, including
90 impaired cellular homeostasis, enzyme inactivation, DNA damage and cell death (27). ROS could also
91 implicate in pathologies, such as cancer, atherosclerosis, diabetes, Down's syndrome, and in
92 neurodegenerative diseases like Parkinson's and Alzheimer's diseases (25, 27, 28). In addition, ROS could
93 serve as the secondary messengers to activate the downstream defense against invaded microorganisms in
94 plants (29, 30), and played an important role in plant secondary metabolism (31). Moreover, ROS could
95 regulate the product synthesis in microorganism, and the yields of xanthan gum produced by *Xanthomonas*
96 *campestris* (29), validamycin A produced by *Streptomyces hygroscopicus* 5008 (31), γ-PGA produced by
97 *Bacillus subtilis* NX-2 (9) and fumonisin produced by *Fusarium verticillioides* (32, 33) were all improved
98 obviously by the ROS induction.

99 *B. licheniformis* WX-02 has been proven to be an efficient γ-PGA producer (13), and several strategies
100 have been conducted to improve γ-PGA synthesis. The yield of γ-PGA was increased 2.3-fold by addition
101 of nitrate in the medium (2). Physicochemical stresses such as heat, osmotic and alkaline could enhance the
102 production of γ-PGA (34, 35). In this study, *ycgM* (encodes PRODH) and *ycgN* (encodes P5CDH) were
103 deleted respectively to analyze the role of proline metabolism on γ-PGA synthesis. The intracellular
104 concentrations of proline, P5C and ATP, ROS levels were analyzed, and the related gene transcriptional
105 levels were measured, to expound the mechanism of *ycgN* deletion on γ-PGA synthesis.

106

107 **RESULTS**

108 **Deletion of *ycgN* improved γ-PGA production in *B. licheniformis***

109 The catabolism of proline was catalyzed by YcgM (PRODH) and YcgN (P5CDH) in *B. licheniformis*

bioRxiv preprint doi: https://doi.org/10.1101/337402; this version posted June 2, 2018. The copyright holder for this preprint (which was not certified by peer review) is the author/funder. All rights reserved. No reuse allowed without permission.

110 WX-02(**Fig. 1**). To investigate the effects of proline metabolism on γ-PGA yield, *ycgM* and *ycgN* were
111 deleted in WX-02, and resulted in strains WXΔ*ycgM* and WXΔ*ycgN*, respectively. These recombinant
112 strains, as well as the control strain WX-02, were cultivated in the γ-PGA production medium. As shown in
113 **Fig. 2A**, the γ-PGA yield of WXΔ*ycgM* was 7.58 g L^{-1}. The γ-PGA yield of WXΔ*ycgN* was 13.91g L^{-1},
114 which was 85.22% higher than that of WX-02 (7.51 g L^{-1}). The yield of γ-PGA from the complementation
115 strain WXΔ*ycgN*-N had no difference with WX-02 (**Fig. 2B**), which confirmed the depletion of *ycgN* along
116 contributes to the increase of γ-PGA yield. To dissect the effect of *ycgN* deletion on γ-PGA synthesis, the
117 *ycgM* and *ycgN* double mutant strain WXΔ*ycgMN* was constructed, which was expected to lack the
118 potential toxic compounds P5C/GSA (**Fig. 1**). Based on our results, the γ-PGA yield of WXΔ*ycgMN* was
119 7.59 g L^{-1}, similar to that of WX-02 (**Fig. 2B**). Furthermore**,** the *ycgM* and *ycgN* genes were overexpressed
120 in WX-02, resulting in WX/*ycgM* and WX/*ycgN*, respectively. As shown in **Fig. 2B,** the γ-PGA yields of
121 WX/*ycgM* (8.49 g L^{-1}) and WX/*ycgN* (8.39 g L^{-1}) were lower than that of control strain WX/pHY300 (11.82
122 g L^{-1}).

123 The γ-PGA yields, biomass, and glucose concentrations during the γ-PGA synthesis were investigated
124 to observe the influences of deletions of *ycgM*, *ycgN*, and double deletion of *ycgMN*. As shown in **Fig. 3,** no
125 remarkable changes of γ-PGA yield, cell growth, or glucose consumption rate were observed among
126 WXΔ*ycgM*, WXΔ*ycgMN* and WX-02. However, the yield of γ-PGA from WXΔ*ycgN* was increased by
127 85.22% (**Fig. 3A**). The lag phase of WXΔ*ycgN* was 4~8 hours longer, and the exponential phase of
128 WXΔ*ycgN* was 4 hours longer. The maximal biomass of WXΔ*ycgN* was 14.07% higher than that of
129 WX-02(**Fig. 3B**). The glucose consumption rate of WXΔ*ycgN* was 1.52 g L^{-1} h^{-1}, which was 22.44% lower
130 than that of WX-02(1.96 g L^{-1} h^{-1}) (**Fig. 3C**).

bioRxiv preprint doi: https://doi.org/10.1101/337402; this version posted June 2, 2018. The copyright holder for this preprint (which was not certified by peer review) is the author/funder. All rights reserved. No reuse allowed without permission.

131

132 **Effect of *ycgN* deficiency on the intracellular proline and P5C concentrations**

133 In *B. licheniformis*, proline was degraded to P5C by YcgM. P5C was then spontaneously changed to
134 GSA, and further converted to glutamate by YcgN (**Fig. 1**). Higher proline levels were observed in both
135 WXΔ*ycgM* (10.04 μmol·gDCW^{-1}) and WXΔ*ycgMN* (8.95 μmol gDCW^{-1}) (**Fig. 4**). Whereas, the proline
136 concentration of WXΔ*ycgN* (6.68 μmol gDCW^{-1}) was similar to that of WX-02 (6.26 μmol·gDCW^{-1}).
137 Meanwhile, the P5C accumulated in WXΔ*ycgN* (19.24 μmol gDCW^{-1}) was significantly higher than that of
138 WX-02 (4.91 μmol gDCW^{-1}) (**Fig. 4**). And the P5C concentration of WXΔ*ycgM* (4.76 μmol gDCW^{-1}) and
139 WXΔ*ycgMN* (4.92 μmol gDCW^{-1}) were comparable to that of WX-02 (**Fig. 4**).

140

141 **The intracellular ROS levels was enhanced in the *ycgN* deletion strain**

142 P5C was reported to be a direct inhibitor of mitochondrial respiration in yeast, which might
143 further lead to intracellular ROS accumulation (24). Thus, we hypothesized that the deletion of *ycgN*
144 might enhance the accumulation of intracellular ROS, which further influenced γ-PGA synthesis. To
145 confirm this hypothesis, the ROS levels of WX-02, WXΔ*ycgM*, WXΔ*ycgN*, and WXΔ*ycgMN* were
146 measured by DCFH method. As shown in **Fig. 5A**, a 1.18-fold increase in fluorescence was detected in
147 WXΔ*ycgN* at 4 h. And the ROS content in WXΔ*ycgN* was found to be significantly decreased after 8 h (**Fig.
148 5A**). The intracellular ROS levels in WXΔ*ycgM* and WXΔ*ycgMN* were 42.60% and 29.38% lower than that
149 of WX-02, respectively (**Fig. 5A**). These results proposed that deletion of *ycgN* induced a transient increase
150 in ROS, which might promote **γ-PGA** synthesis.

151

bioRxiv preprint doi: https://doi.org/10.1101/337402; this version posted June 2, 2018. The copyright holder for this preprint (which was not certified by peer review) is the author/funder. All rights reserved. No reuse allowed without permission.

152 **The *ycgN*-dependent ROS signal contributed to γ-PGA synthesis**

153 ROS has been reported to promote γ-PGA synthesis capability in *B. subtilis* NX-2 previously (9). Thus,
154 the transiently increased ROS level observed in WXΔ*ycgN* was proposed to be the primary cause of γ-PGA
155 enhancement. To test this hypothesis, n-acetylcysteine (NAC, antioxidant) (10 mmol L^{-1}), a widely used
156 antioxidant agent, was added into the medium to neutralize the ROS production. In the present of NAC, the
157 ROS level of WXΔ*ycgN* was similar to that of WX-02 at 4 h (**Fig. 5B**). The γ-PGA yield of WXΔ*ycgN* was
158 7.06 g L^{-1}, which is near to WX-02 (**Fig. 5C**). To further verify that ROS would promote γ-PGA synthesis
159 in *B. licheniformis* WX-02, H_2O_2 was supplied as a simple mean to increase the intrinsic ROS levels. Our
160 result implied that addition of 10 mmol L^{-1} H_2O_2 could increase the γ-PGA yield (13.88 g L^{-1}) by 77.72%
161 (**Fig. S1**). Collectively, our results suggested that the increase of ROS induced by the deletion of *ycgN*
162 might contribute to the enhancement of γ-PGA yield in WXΔ*ycgN*. Overproduction of ROS has been
163 reported to cause damage of intracellular biomolecules, such as proteins, DNA and lipids, which was not
164 conducive to the cell growth (25, 39, 40). Consequently, WXΔ*ycgN* exhibited a slight growth defect and the
165 extended lag phase, compared with those of WX-02.

166 **Effect of *ycgN* deletion on the intracellular ATP concentration**

167 ATP supply is essential for product synthesis, as well as in γ-PGA (15). As show in **Fig. 5D**, the
168 intracellular ATP concentration of WXΔ*ycgN* was 11.875 μmol gDCW^{-1}, increased by 24.40% compared to
169 that of WX-02 (9.55 μmol gDCW^{-1}). The ATP concentrations of WXΔ*ycgM* and WXΔ*ycgMN* were 6.65
170 μmol gDCW^{-1} and 10.19 μmol gDCW^{-1}, respectively. These results indicate that deletion of *ycgN* improved
171 the intracellular ATP supply, which was beneficial for γ-PGA synthesis.

172

bioRxiv preprint doi: https://doi.org/10.1101/337402; this version posted June 2, 2018. The copyright holder for this preprint (which was not certified by peer review) is the author/funder. All rights reserved. No reuse allowed without permission.

173 **Transcriptional levels of genes related to γ-PGA synthesis in *ycgN* mutant strain**

174 The general stress response of *B. licheniformis* is controlled by the σ^B transcription factor encoded by
175 *sigB* (41). To approve that deletion of *ycgN* could cause oxidative stress in *B. licheniformis* WX-02, the
176 transcription level of *sigB* was determined in WXΔ*ycgN*. As shown in **Fig. 6**, the relative expression level
177 of the gene *sigB* in WXΔ*ycgN* was increased to 13.15.

178 To investigate the roles of YcgN on expression of genes involved in γ-PGA synthesis, the transcription
179 levels of *degU*, *swrA*, *pgsB*, and *pgsC* were analyzed in WXΔ*ycgN*. As shown in **Fig. 6**, the transcriptional
180 levels of genes *pgsB* and *pgsC*, which are responsible for γ-PGA biosynthesis, were increased by 49.52- and
181 19.31-fold, respectively. The expression of *pgs* operon is activated by SwrA and phosphorylated DegU
182 (DegU-P) (4). Accordingly, the transcriptional levels of genes *degU* and *swrA* were enhanced by 1.79- and
183 11.92-fold, respectively (**Fig. 6**). Also, the transcriptional levels of relevant genes in TCA cycle, including
184 *citZ* (encodes citrate synthase) and *icd* (encodes isocitrate dehydrogenase) were verified, as the precursor of
185 γ-PGA glutamate can be synthesized from α-Ketoglutaric acid. And the expression levels of both genes
186 were increased by 8.36- and 13.93- fold in WXΔ*ycgN*, respectively (**Fig. 6**).

187

188 **Discussion**

189 Proline is a multifunctional amino acid which can be used as carbon, nitrogen and energy source (18).
190 Also, it plays an important role in protecting against osmotic and oxidative stresses, since it is a compatible
191 solute and a free-radical scavenger (42). In addition, proline catabolism has been found to be involved in
192 protection of intracellular redox homeostasis and virulence in microorganisms (26, 43). In this study, we
193 demonstrated that the deletion of *ycgN* significantly enhanced γ-PGA production in *B. licheniformis* WX-02,

bioRxiv preprint doi: https://doi.org/10.1101/337402; this version posted June 2, 2018. The copyright holder for this preprint (which was not certified by peer review) is the author/funder. All rights reserved. No reuse allowed without permission.

194 and this phenomenon was disappeared in the complementation strain. Besides, the increases of P5C
195 concentration, ROS and intracellular ATP concentration were observed in *ycgN* deletion strain. These
196 results indicated that proline metabolism is valuable in regulating γ-PGA synthesis, and the transient
197 increase in ROS level seemed to be required for the enhancement of γ-PGA synthesis caused by deletion of
198 *ycgN*.

199 Briefly, the degradation of proline to glutamate is catalyzed by PRODH and P5CDH. Glutamate can
200 be converted to α-ketoglutarate (α-KG) by a transamination, and then oxidized in the TCA cycle along with
201 ATP generation (**Fig.1**). In the previous research, knocking out of P5CDH encoded gene *Ldp5cdh* in the
202 Colorado potato beetle *Leptinotarsa decemlineata* could significantly reduce the ATP content, and further
203 inhibit flight capacity (42). This study implied that deletion of *ycgN* in *B. licheniformis* WX-02 led to an
204 85.22% increase of γ-PGA yield. One explanation is that deletion of *ycgN* prevents the pathway of proline
205 oxidation, and then reduces ATP content. However, the catabolism of proline was interrupted in *ycgM*
206 mutant and *ycgMN* double mutant strains (Fig. 1), the γ-PGA yield exhibited no difference from the
207 wild-type. Moreover, the ATP content of *ycgN* deletion strain was significantly higher than that of wild-type
208 strain and other mutants. Thus, the interrupting of proline oxidation and ATP generation might not be the
209 main reason for the enhancement of γ-PGA yield obtained in the *ycgN* deletion strain.

210 Based on our results, the enhancement of γ-PGA in WXΔ*ycgN* was related to the ROS accumulation
211 (**Fig. 5**). In the previous researches, impaired P5C dehydrogenase activity was supposed to induce ROS
212 generation by causing intense P5C-proline cycling in animals, plants and fungus (26). The oxidation of
213 proline to P5C by FAD dependent-ProDH provides an excess of electrons to the mitochondrial electron
214 transport chain and enhances ROS accumulation (17, 26, 44). P5CDH would prevent the excessive

bioRxiv preprint doi: https://doi.org/10.1101/337402; this version posted June 2, 2018. The copyright holder for this preprint (which was not certified by peer review) is the author/funder. All rights reserved. No reuse allowed without permission.

215 producing and accumulation of ROS by converting P5C to glutamate irreversibly (44). However,
216 overexpression of *ycgM* did not improve γ-PGA production in WX-02, indicating that the increase of
217 γ-PGA production in WX-02Δ*ycgN* was not attributed to the proline-P5C cycling. Another interpretation
218 was that the effects of *ycgN* mutation were mediated by P5C. Consistently, an increase of P5C was detected
219 in *ycgN* mutant but not in other mutants. Hence, the improvement of γ-PGA production in *ycgN* deletion
220 strain might due to the P5C or P5C-derived signals.

221 Formaldehyde and acetaldehyde, which containing the aldehyde group, had been proved to be able to
222 impair mitochondrial function and then generate ROS (45, 46). P5C attacks the mitochondrial respiratory
223 chain and induces a burst of superoxide anions from the mitochondria in *Saccharomyces cerevisiae* R1278b
224 (24). P5C is also a primary inducer of p53-mediated apoptosis and ROS-dependent autophagy proposed in
225 mammals (47). In plants, P5CDH infection resulted in P5C accumulation and induced ROS burst (48, 49).
226 Thus, it might be reasonable that P5C or, more likely, its equilibrium compound GSA with an unstable
227 aldehyde group, contributed to the γ-PGA enhancement by inducing ROS burst via inhibiting the
228 respiratory chain. Based on our results, a transient increase of ROS was observed at earlier time points in
229 WX-02Δ*ycgN* mutants, but not in WX-02, WX-02Δ*ycgM* or WX-02Δ*ycgMN*.

230 γ-PGA is a homopolymer of glutamate with diverse biochemical properties (4). Several organisms
231 secrete γ-PGA into the environment for sequestration of toxic metal ions or decreasing high local salt
232 concentrations, enabling them to survive in adverse conditions (4). In our previous researches, the γ-PGA
233 synthesis capability was strengthened when the strains were cultured in the stress conditions, such as high
234 salt, high temperature, caustic alkali, and ultrasonic shock (20). Here, it was found that the γ-PGA synthesis
235 of WX-pHY300 was increased by 57.40% compared with that of WX-02 (**Fig. 2**), which was in line with

bioRxiv preprint doi: https://doi.org/10.1101/337402; this version posted June 2, 2018. The copyright holder for this preprint (which was not certified by peer review) is the author/funder. All rights reserved. No reuse allowed without permission.

236 the previous studies. Since the plasmid was supposed to exhibit metabolic burden on the host and affected
237 host gene expression and phenotype, it was suspicious that the enhancement of γ-PGA synthesis in
238 WX-pHY300 could be an element of response or adaptation response against stress caused by pHY300
239 (50-53). According to this study, oxidative stress increased γ-PGA production in WX-02 by *ycgN* deletion
240 or H_2O_2 addition. The addition of n-acetylcysteine decreased the γ-PGA yield of WXΔ*ycgN* to the level
241 near that of WX-02. Thus, γ-PGA synthesis could be an element for adaptation response against oxidative
242 stress.

243 ROS has been proposed to act as the secondary messenger and regulate many processes at the
244 transcriptional level (19, 31, 54, 55). The global regulator OxyR was reported to react with H_2O_2 and form a
245 disulfide bond between Cys199 and Cys208, resulting in the transcriptional activation of OxyR regulator in
246 *E. coli* (19). In *B. subtilis*, ROS, induced by high shear stress, altered the transcription of general protein
247 Sigma B and Ctc, and then regulated the suppression of sporulation (31). The transcription levels of *degU*,
248 *swrA*, and *pgsB* which are related to γ-PGA biosynthesis were markedly increased in the *ycgN* deletion
249 strain. In recent researches, DegU was proposed to be under control of the redox-sensing regulators
250 ClpXP/Spx (56-58). Therefore, the intracellular ROS, induced by *ycgN* deletion, promoted the transcription
251 level of *degU* probably by activating Spx. Also, the transcription of *swrA* was significantly improved in
252 WXΔ*ycgN*, and the improvement of SwrA might cooperate with DegU to active the expression of *pgs*
253 operon and promote γ-PGA synthesis (**Fig.7**).

254

255 **Conclusion**

256 The role of proline metabolism on γ-PGA synthesis is analyzed in this work. Based on our results,

bioRxiv preprint doi: https://doi.org/10.1101/337402; this version posted June 2, 2018. The copyright holder for this preprint (which was not certified by peer review) is the author/funder. All rights reserved. No reuse allowed without permission.

257 γ-PGA synthesis in *B. licheniformis* WX-02 was enhanced by the deletion of *ycgN*, which yield was 85.22%
258 higher than that of wild-type strain. Secondly, the P5C concentration of WX-02Δ*ycgN* was 2.92-fold
259 increased, which resulted in the intracellular ROS accumulation. These results illustrate the importance of
260 P5C dehydrogenase in regulating γ-PGA production, and it provides valuable information for metabolic
261 engineering of high-yield γ-PGA strain of *B. licheniformis*.

262 **MATERIALS AND METHODS**

263 **Bacterial strains, media and culture conditions**

264 The strains and plasmids used in this work are listed in **Table 1**. *B. licheniformis* and *Escherichia coli*
265 were cultured at 37 ℃ in Luria-Bertani (LB) broth (1% tryptone, 0.5% yeast extract, 1% NaCl and pH 7.2).
266 The seed culture of *B. licheniformis* was prepared in a 250 mL flasks containing 50 mL LB medium, and
267 incubated at 37 ℃ in a rotatory shaker (180 rpm) for 10 h until OD_{600} reached 4.6~5.0. The seed culture
268 (1.50 mL) was inoculated into 250 mL flask containing 50 mL γ-PGA production medium (g L^{-1}: glucose
269 60, sodium nitrate 10, sodium citrate 10, NH_4Cl 8, $CaCl_2$ 1, $K_2HPO_4 \cdot 3H_2O$ 1, $MgSO_4 \cdot 7H_2O$ 1,
270 $ZnSO_4 \cdot 7H_2O$ 1, $MnSO_4 \cdot 7H_2O$ 0.15 and $FeCl_3 \cdot 6H_2O$ 0.04), and shaken at 37 ℃ and 180 rpm for 32 h. All
271 the fermentation experiments were performed in three replicates. The antibiotics kanamycin and
272 tetracycline were added into *B. licheniformis* cultures at the final concentration of 20 mg L^{-1} when
273 necessary. Kanamycin and Ampicillin were added to *E. coli* cultures at final concentrations of 20 mg L^{-1}
274 and 50 mg L^{-1}, respectively.

275 **Construction of plasmids and strains**

276 DNA manipulations were performed according to our previous researches (13, 36). The construction
277 procedure of *ycgN* deficient strain was served as an example. Briefly, the homology arms of gene *ycgN*

bioRxiv preprint doi: https://doi.org/10.1101/337402; this version posted June 2, 2018. The copyright holder for this preprint (which was not certified by peer review) is the author/funder. All rights reserved. No reuse allowed without permission.

278 were amplified from chromosomal DNA of *B. licheniformis* WX-02 with primers *ycgN*-A-F/ *ycgN*-A-R and
279 *ycgN*-B-F/ *ycgN*-B-R (**Table 2**), respectively. The resulting fragments were purified and ligated by Splicing
280 Overlapping Extension PCR (SOE-PCR) with the primers *ycgN*-A-F and *ycgN*-B-R. The fused fragment
281 was digested with *Bam*HI and *Xba*I, and inserted into T2(2)-Ori, named T2-*ycgN*(13, 36).

282 Then, the recombinant vector T2-*ycgN* was transformed into *B. licheniformis* WX-02 by
283 high-osmolality electroporation, according to our previously reported method (37). The transformants were
284 selected by kanamycin resistance and verified by PCR with the primers T2-F and T2-R. Then, the positive
285 colony was cultured in LB medium containing kanamycin (20 mg L^{-1}) at 45 ℃ for 8 h to obtain the
286 single-crossover recombinants, and the double-crossover recombinants were screened after serial subculture
287 of single-cross recombinants in LB medium at 37 ℃. The kanamycin sensitive colonies resulting from the
288 double-crossover event were selected, and confirmed by DNA sequencing with the primers Δ*ycgN*-F and
289 Δ*ycgN*-R. The positive mutant strain was designated as WXΔ*ycgN*. The complement of *ycgN* mutation was
290 generated by introducing the gene *ycgN* into WXΔ*ycgN* at the *amyL* locus, and named as WX Δ*ycgN*-N.
291 Similarly, the *ycgM* deletion, *ycgM* and *ycgN* double deletion strains were constructed with the same
292 method, named WXΔ*ycgM* and WXΔ*ycgMN*, respectively.

293 The gene expression vector was constructed according to our previously reported method (13). Briefly,
294 the P_{srf} promoter (938306) of *B. subtilis* 168, gene *ycgN* (16054241) and the *amyL* terminator (3031010) of
295 *B. licheniformis* WX-02 were amplified by the corresponding primers. The amplified fragments were fused
296 by SOE-PCR. The fused fragment was inserted into pHY300PLK at the restriction enzyme sites
297 *Bam*HI/*Xba*I, resulting in the *ycgN* expression vector, named pHY-*ycgN*. The vectors pHY300PLK and
298 pHY-*ycgN* were then transformed into *B. licheniformis* WX-02, and the recombinant strains were named

bioRxiv preprint doi: https://doi.org/10.1101/337402; this version posted June 2, 2018. The copyright holder for this preprint (which was not certified by peer review) is the author/funder. All rights reserved. No reuse allowed without permission.

299 WX/pHY300 and WX/*ycgN*, respectively. The strain over-expressing *ycgM* was constructed using the
300 similar method, and the recombinant strain was named as WX/*ycgM*.

301 **Analytical methods**

302 The cell biomass was detected by measuring the absorbance at 600 nm. Briefly, the volume of 2 mL
303 culture broth was centrifuged at 13 700×*g* for 10 min. The cell pellet was washed three times with 0.85%
304 NaCl solution and re-suspended. The optical density at 600 nm (OD_{600}) was measured by a
305 spectrophotometer (Bio-Rad, USA) (38). To determine the γ-PGA concentration, three-fold volume of
306 ethanol was added into the supernatant, and centrifuged at 9540×*g* for 10 min, and resolved with distilled
307 water. The γ-PGA concentration was measured by the method of HPLC according to our previous research
308 (14). The concentration of residual glucose was detected by a SBA-40C biosensor analyzer (Institute of
309 Biology, Shandong Province Academy of Sciences, P. R. China) according to the manufacturer's
310 instructions.

311 **Determination of proline and P5C concentrations**

312 The cells at logarithmic phase was harvested by centrifugation, washed twice with 0.85% NaCl, and
313 extracted overnight in 5 mL 3% (w/v) aqueous 5-sulphosalicylic acid. Precipitated protein and other debris
314 were removed by centrifugation at 15 000×*g*, 5 min. To determine the proline content, the volume of 2.0
315 mL cell extract was reacted with 2.0 mL glacial acetic acid and 2.0 mL acid-ninhydrin (2.5 g ninhydrin was
316 dissolved in the mixed solution of 60 mL glacial acetic acid and 40 mL 6 M phosphoric acid) at 100 ℃ for 1
317 h. Samples were then plunged into ice to stop the reaction, and extracted with 5 mL toluene. The
318 absorbance of toluene phase was separated and measured at 520 nm. The proline concentration was
319 calculated according to the standard curve made by proline standard.

bioRxiv preprint doi: https://doi.org/10.1101/337402; this version posted June 2, 2018. The copyright holder for this preprint (which was not certified by peer review) is the author/funder. All rights reserved. No reuse allowed without permission.

320 To determine the P5C content, the volume of 1 mL cell extract was added with 0.1 mL trichloroacetic
321 acid, and then 0.5 mL 6 mg mL^{-1} *o*-aminobenzaldehyde (2-AB) was added to the mixture, and insulated at
322 37 ℃ for 1 h. The mixture was centrifuged at 10 000×*g* for 10 min. The absorbance of the supernatant was
323 measured at 443 nm, in an l-cm light path. The pyrroline-5-carbosylate concentration (c) was calculated
324 according to Lambert-Beer law: A=Ɛ*l*c. The millimolar extinction coefficient (Ɛ) of the
325 P5C-oaminobenzaldehyde complex is 2.71 mM^{-1} cm^{-1} (18).

326 **Determination of ROS**

327 The intracellular ROS levels were measured by the Reactive Oxygen species Assay Kit (Nanjing
328 Jiancheng Bioengineering Institute, P.R. China) according to the manufacturer's instructions. In brief, the
329 cells were collected by centrifugation at 13 700×*g* for 10 min, and re-suspended with PBS solution and
330 diluted to OD_{600} = 1.0. The volume of 1 mL cell suspension was added with 10 mM DCFH-DA, and
331 incubated at 37 ℃ for 30 min. The cells were then re-suspended in 1 mL PBS solution, and the relative
332 fluorescence was measured at excitation and emission wavelengths of 485 and 525 nm by using a
333 fluorescence spectrophotometer (Shimadzu, Japan). Untreated cells were used as reference, and the relative
334 ROS amounts were showed by fluorescence intensity (9).

335 **Determination of ATP concentrations**

336 The intracellular ATP concentration was quantified by a ATP assay kit (Beyotime, China) according to
337 the manufacturer's instructions (2). Briefly, the cells were lysed by the lysis buffer, and then centrifuged at
338 12 000×*g* at 4 ℃ for 5 min, the volume of 20 μL supernatant was mixed with 100 μL luciferase reagent, and
339 the luminance was measured by a luminometer. The ATP concentration was calculated according to the
340 standard curve made by ATP standard, and defined as the content of ATP to the cell dry weight. All assays

bioRxiv preprint doi: https://doi.org/10.1101/337402; this version posted June 2, 2018. The copyright holder for this preprint (which was not certified by peer review) is the author/funder. All rights reserved. No reuse allowed without permission.

341 were performed in triplicate.

342 **Quantitative real-time PCR (qRT-PCR)**

343 The qRT-PCR assay was conducted according to our previous reported method (13, 36). Briefly, the
344 total RNA was extracted by using the Trizol Reagent (Invitrogen, USA), and DNase I enzyme (TaKaRa,
345 Japan) was applied to degrade trace DNA. The first strand of cDNA was amplified from 0.5 μg of total
346 RNA using the RevertAid First Strand cDNA Synthesis Kit (Thermo, USA) with random primers. The
347 real-time PCR was performed with the Maxima® SYBR Green/ROX qPCR Master Mix (Thermo)
348 following the manufacturer's instructions. The primers used for amplifying the corresponding genes were
349 listed in **Table S1** (seeing in the Supplementary Material), and 16 S rDNA was used as the reference gene
350 to normalize the data. All the experiments were performed in triplicate. The gene expression levels of
351 recombinant strain were compared with those of wild-type strain after normalization to the reference gene.

352

353 **Competing interests**

354 The authors declare that they have no competing interests.

355 **Athour's contribution**

356 B Li, Z He and S Chen designed the study. B Li carried out the molecular biology studies and
357 construction of engineering strains. B Li and S Hu carried out the fermentation studies. B Li, D Cai, A Zhu
358 and S Chen analyzed the data and wrote the manuscript. All authors read and approved the final manuscript.

359 **Acknowledgments**

360 This work was supported by the National Program on Key Basic Research Project (973 Program, No.
361 2015CB150505), the Technical Innovation Special Fund of Hubei Province (2018ACA149) and the
362 Science and Technology Program of Wuhan (20160201010086).

bioRxiv preprint doi: https://doi.org/10.1101/337402; this version posted June 2, 2018. The copyright holder for this preprint (which was not certified by peer review) is the author/funder. All rights reserved. No reuse allowed without permission.

363 **Supporting Information**

364 All the primers sequences for RT-qPCR were listed in **Table S1 and Table S2**. This information was

365 available free of charge via the Internet: http://aem.asm.org/.

366

367

368 **Reference**

369 1. Candela T, Fouet A. 2006. Poly-gamma-glutamate in bacteria. Mol Microbiol 60:1091-1098.
370 2. Li X, Gou X, Long D, Ji Z, Hu L, Xu D, Liu J, Chen S. 2014. Physiological and metabolic
371 analysis of nitrate reduction on poly-gamma-glutamic acid synthesis in *Bacillus licheniformis*
372 WX-02. Arch Microbiol 196:791-799.
373 3. Tian G, Fu J, Wei X, Ji Z, Ma X, Qi G, Chen S. 2014. Enhanced expression of *pgdS* gene for high
374 production of poly-γ-glutamic aicd with lower molecular weight in *Bacillus licheniformis*WX-02.
375 J Chem Technol Biotechnol 89:1825-1832.
376 4. Ogunleye A, Bhat A, Irorere VU, Hill D, Williams C, Radecka I. 2015. Poly-gamma-glutamic acid:
377 production, properties and applications. Microbiology 161:1-17.
378 5. Shih IL, Van YT. 2001. The production of poly-(gamma-glutamic acid) from microorganisms and
379 its various applications. Bioresour Technol 79:207-225.
380 6. Tan S, Meng Y, Su A, Zhang C, Ren Y. 2016. Draft Genome Sequence of *Bacillus subtilis subsp*.
381 natto Strain CGMCC 2108, a High Producer of Poly-gamma-Glutamic Acid. Genome Announc 4.
382 7. Mitsunaga H, Meissner L, Palmen T, Bamba T, Buchs J, Fukusaki E. 2016. Metabolome analysis
383 reveals the effect of carbon catabolite control on the poly(gamma-glutamic acid) biosynthesis of
384 *Bacillus licheniformis* ATCC 9945. J Biosci Bioeng 121:413-419.
385 8. Meng Y, Dong G, Zhang C, Ren Y, Qu Y, Chen W. 2016. Calcium regulates glutamate
386 dehydrogenase and poly-gamma-glutamic acid synthesis in *Bacillus natt*o. Biotechnol Lett
387 38:673-679.
388 9. Tang B, Zhang D, Li S, Xu Z, Feng X, Xu H. 2016. Enhanced poly(gamma-glutamic acid)
389 production by H_2O_2-induced reactive oxygen species in the fermentation of *Bacillus subtilis* NX-2.
390 Biotechnol Appl Biochem 63:625-632.
391 10. Feng J, Gao W, Gu Y, Zhang W, Cao M, Song C, Zhang P, Sun M, Yang C, Wang S. 2014.
392 Functions of poly-gamma-glutamic acid (gamma-PGA) degradation genes in gamma-PGA
393 synthesis and cell morphology maintenance. Appl Microbiol Biotechnol 98:6397-6407.
394 11. Feng J, Gu Y, Quan Y, Cao M, Gao W, Zhang W, Wang S, Yang C, Song C. 2015. Improved
395 poly-gamma-glutamic acid production in *Bacillus amyloliquefaciens* by modular pathway
396 engineering. Metab Eng 32:106-115.
397 12. Jiang F, Qi G, Ji Z, Zhang S, Liu J, Ma X, Chen S. 2011. Expression of *glr* gene encoding
398 glutamate racemase in *Bacillus licheniformis* WX-02 and its regulatory effects on synthesis of

bioRxiv preprint doi: https://doi.org/10.1101/337402; this version posted June 2, 2018. The copyright holder for this preprint (which was not certified by peer review) is the author/funder. All rights reserved. No reuse allowed without permission.

399 poly-gamma-glutamic acid. Biotechnol Lett 33:1837-1840.

400 13. Cai D, He P, Lu X, Zhu C, Zhu J, Zhan Y, Wang Q, Wen Z, Chen S. 2017. A novel approach to
401 improve poly-gamma-glutamic acid production by NADPH Regeneration in *Bacillus licheniformis*
402 WX-02. Sci Rep 7:43404.

403 14. Tian G, Wang Q, Wei X, Ma X, Chen S. 2017. Glutamate dehydrogenase (RocG) in *Bacillus*
404 *licheniformis* WX-02: Enzymatic properties and specific functions in glutamic acid synthesis for
405 poly-gamma-glutamic acid production. Enzyme Microb Technol 99:9-15.

406 15. Cai D, Hu S, Chen Y, Liu L, Yang S, Ma X, Chen S. 2018. Enhanced Production of
407 Poly-gamma-glutamic acid by Overexpression of the Global Anaerobic Regulator Fnr in *Bacillus*
408 *licheniformis* WX-02. Appl Biochem Biotechnol doi:10.1007/s12010-018-2693-7.

409 16. Zhan Y, Zhu C, Sheng B, Cai D, Wang Q, Wen Z, Chen S. 2017. Improvement of glycerol
410 catabolism in *Bacillus licheniformis* for production of poly-gamma-glutamic acid. Appl Microbiol
411 Biotechnol 101:7155-7164.

412 17. Liang X, Zhang L, Natarajan SK, Becker DF. 2013. Proline mechanisms of stress survival.
413 Antioxid Redox Signal 19:998-1011.

414 18. Moses S, Sinner T, Zaprasis A, Stoveken N, Hoffmann T, Belitsky BR, Sonenshein AL, Bremer E.
415 2012. Proline utilization by *Bacillus subtilis*: uptake and catabolism. J Bacteriol 194:745-758.

416 19. Zhang L, Alfano JR, Becker DF. 2015. Proline metabolism increases *katG* expression and
417 oxidative stress resistance in *Escherichia coli*. J Bacteriol 197:431-440.

418 20. Guo J, Cheng G, Gou X, Xing F, Li S, Han Y, Wang L, Song J, Shu C, Chen S, Chen L. 2015.
419 Comprehensive transcriptome and improved genome annotation of *Bacillus licheniformis* WX-02.
420 FEBS Lett 589:2372-2381.

421 21. Natarajan SK, Zhu WD, Liang XW, Zhang L, Demers AJ, Zimmerman MC, Simpson MA, Becker
422 DF. 2012. Proline dehydrogenase is essential for proline protection against hydrogen
423 peroxide-induced cell death. Free Radical Biol Med 53:1181-1191.

424 22. Hoper D, Bernhardt J, Hecker M. 2006. Salt stress adaptation of *Bacillus subtilis*: a physiological
425 proteomics approach. Proteomics 6:1550-1562.

426 23. Khavari-Nejad RA, Band RS, Najafi F, Nabiuni M, Gharari Z. 2013. The role of Pro-P5C Cycle in
427 *chs* mutants of *Arabidopsis* under cold stress. Russ J Plant Physiol 60:375-382.

428 24. Nishimura A, Nasuno R, Takagi H. 2012. The proline metabolism intermediate
429 Delta1-pyrroline-5-carboxylate directly inhibits the mitochondrial respiration in budding yeast.
430 FEBS Lett 586:2411-2416.

431 25. Singh S, Brocker C, Koppaka V, Chen Y, Jackson BC, Matsumoto A, Thompson DC, Vasiliou V.
432 2013. Aldehyde dehydrogenases in cellular responses to oxidative/electrophilic stress. Free Radic
433 Biol Med 56:89-101.

434 26. Lee IR, Lui EYL, Chow EWL, Arras SDM, Morrow CA, Fraser JA. 2013. Reactive Oxygen
435 Species Homeostasis and Virulence of the Fungal Pathogen Cryptococcus neoformans Requires an
436 Intact Proline Catabolism Pathway. Genetics 194:421-433.

437 27. Temple MD, Perrone GG, Dawes IW. 2005. Complex cellular responses to reactive oxygen species.
438 Trends Cell Biol 15:319-326.

439 28. Zuo L, Hemmelgarn BT, Chuang CC, Best TM. 2015. The Role of Oxidative Stress-Induced

bioRxiv preprint doi: https://doi.org/10.1101/337402; this version posted June 2, 2018. The copyright holder for this preprint (which was not certified by peer review) is the author/funder. All rights reserved. No reuse allowed without permission.

440 Epigenetic Alterations in Amyloid-beta Production in Alzheimer's Disease. Oxid Med Cell Longev
441 2015:604658.
442 29. Rao Y, Sureshkumar GK. 2001. Improvement in bioreactor productivities using free radicals:
443 HOCl-induced overproduction of xanthan gum from *Xanthomonas campestris* and its mechanism.
444 Biotechnol Bioeng 72:62-68.
445 30. Coll NS, Danon A, Meurer J, Cho WK, Apel K. 2009. Characterization of *soldat*8, a suppressor of
446 singlet oxygen-induced cell death in *Arabidopsis* seedlings. Plant Cell Physiol 50:707-718.
447 31. Wei Z, Bai L, Deng Z, Zhong J. 2011. Enhanced production of validamycin A by H_2O_2-induced
448 reactive oxygen species in fermentation of *Streptomyces hygroscopicus* 5008. Bioresour Technol
449 102:1783-1787.
450 32. Ponts N, Pinson-Gadais L, Verdal-Bonnin MN, Barreau C, Richard-Forget F. 2006. Accumulation
451 of deoxynivalenol and its 15-acetylated form is significantly modulated by oxidative stress in
452 liquid cultures of *Fusarium graminearum*. Fems Microbiology Letters 258:102-107.
453 33. Ferrigo D, Raiola A, Bogialli S, Bortolini C, Tapparo A, Causin R. 2015. In Vitro Production of
454 Fumonisins by *Fusarium verticillioides* under Oxidative Stress Induced by H_2O_2. J Agric Food
455 Chem 63:4879-4885.
456 34. Wang J, Yuan H, Wei X, Chen J, Chen S. 2016. Enhancement of poly-γ-glutamic acid production
457 by alkaline pH stress treatment in *Bacillus licheniformis* WX-02. J Chem Technol Biotechnol
458 91:2399-2403.
459 35. Wei X, Tian G, Ji Z, Chen S. 2015. A new strategy for enhancement of poly-γ-glutamic acid
460 production by multiple physicochemical stresses in *Bacillus licheniformis*. J Chem Technol
461 Biotechnol 90:709-713.
462 36. Qiu Y, Xiao F, Wei X, Wen Z, Chen S. 2014. Improvement of lichenysin production in *Bacillus*
463 *licheniformis* by replacement of native promoter of lichenysin biosynthesis operon and medium
464 optimization. Appl Microbiol Biotechnol 98:8895-8903.
465 37. Qi G, Kang Y, Li L, Xiao A, Zhang S, Wen Z, Xu D, Chen S. 2014. Deletion of
466 meso-2,3-butanediol dehydrogenase gene *budC* for enhanced D-2,3-butanediol production in
467 *Bacillus licheniformis*. Biotechnol Biofuels 7:16.
468 38. Wei X, Ji Z, Chen S. 2010. Isolation of halotolerant *Bacillus licheniformis* WX-02 and regulatory
469 effects of sodium chloride on yield and molecular sizes of poly-gamma-glutamic acid. Appl
470 Biochem Biotechnol 160:1332-1340.
471 39. Si M, Zhang L, Yang Z, Xu Y, Liu Y, Jiang C, Wang Y, Shen X, Liu S. 2014. NrdH Redoxin
472 enhances resistance to multiple oxidative stresses by acting as a peroxidase cofactor in
473 *Corynebacterium glutamicum*. Appl Environ Microbiol 80:1750-1762.
474 40. Man Z, Rao Z, Xu M, Guo J, Yang T, Zhang X, Xu Z. 2016. Improvement of the intracellular
475 environment for enhancing l-arginine production of *Corynebacterium glutamicum* by inactivation
476 of H_2O_2-forming flavin reductases and optimization of ATP supply. Metab Eng 38:310-321.
477 41. Brody MS, Price CW. 1998. Bacillus licheniformis *sigB* operon encoding the general stress
478 transcription factor sigma B. Gene 212:111-118.
479 42. Wan P, Fu K, Lu F, Wang X, Guo W, Li G. 2015. Knocking down a putative Delta(1)
480 -pyrroline-5-carboxylate dehydrogenase gene by RNA interference inhibits flight and causes adult

bioRxiv preprint doi: https://doi.org/10.1101/337402; this version posted June 2, 2018. The copyright holder for this preprint (which was not certified by peer review) is the author/funder. All rights reserved. No reuse allowed without permission.

481 lethality in the Colorado potato beetle Leptinotarsa decemlineata (Say). Pest Manag Sci
482 71:1387-1396.
483 43. Yao Z, Zou C, Zhou H, Wang J, Lu L, Li Y, Chen B. 2013.
484 Delta(1)-pyrroline-5-carboxylate/glutamate biogenesis is required for fungal virulence and
485 sporulation. PLoS One 8:e73483.
486 44. Miller G, Honig A, Stein H, Suzuki N, Mittler R, Zilberstein A. 2009. Unraveling
487 delta1-pyrroline-5-carboxylate-proline cycle in plants by uncoupled expression of proline
488 oxidation enzymes. J Biol Chem 284:26482-26492.
489 45. Teng S, Beard K, Pourahmad J, Moridani M, Easson E, Poon R, O'Brien PJ. 2001. The
490 formaldehyde metabolic detoxification enzyme systems and molecular cytotoxic mechanism in
491 isolated rat hepatocytes. Chem Biol Interact 130-132:285-296.
492 46. Farfan Labonne BE, Gutierrez M, Gomez-Quiroz LE, Konigsberg Fainstein M, Bucio L, Souza V,
493 Flores O, Ortiz V, Hernandez E, Kershenobich D, Gutierrez-Ruiz MC. 2009.
494 Acetaldehyde-induced mitochondrial dysfunction sensitizes hepatocytes to oxidative damage. Cell
495 Biol Toxicol 25:599-609.
496 47. Hu CAA, Donald SP, Yu J, Lin W, Liu Z, Steel G, Obie C, Valle D, Phang JM. 2007.
497 Overexpression of proline oxidase induces proline-dependent and mitochondria-mediated
498 apoptosis. Mol Cel Biochem 295:85-92.
499 48. Monteoliva MI, Rizzi YS, Cecchini NM, Hajirezaei MR, Alvarez ME. 2014. Context of action of
500 proline dehydrogenase (ProDH) in the Hypersensitive Response of *Arabidopsis*. BMC Plant Biol
501 14:21.
502 49. Deuschle K, Funck D, Forlani G, Stransky H, Biehl A, Leister D, van der Graaff E, Kunze R,
503 Frommer WB. 2004. The role of [Delta]1-pyrroline-5-carboxylate dehydrogenase in proline
504 degradation. Plant Cell 16:3413-3425.
505 50. Rosch TC, Golman W, Hucklesby L, Gonzalez-Pastor JE, Graumann PL. 2014. The presence of
506 conjugative plasmid pLS20 affects global transcription of Its *Bacillus subtilis* host and confers
507 beneficial stress resistance to cells. Appl Environ Microbiol 80:1349-1358.
508 51. Mairhofer J, Scharl T, Marisch K, Cserjan-Puschmann M, Striedner G. 2013. Comparative
509 transcription profiling and in-depth characterization of plasmid-based and plasmid-free
510 *Escherichia coli* expression systems under production conditions. Appl Environ Microbiol
511 79:3802-3812.
512 52. Hong H, Jung J, Park W. 2014. Plasmid-encoded tetracycline efflux pump protein alters bacterial
513 stress responses and ecological fitness of *Acinetobacter oleivorans*. PLoS One 9:e107716.
514 53. Yu W, Chen Z, Shen L, Wang Y, Li Q, Yan S, Zhong C, He N. 2016. Proteomic profiling of
515 *Bacillus licheniformis* reveals a stress response mechanism in the synthesis of extracellular
516 polymeric flocculants. Biotechnol Bioeng 113:797-806.
517 54. D'Autreaux B, Toledano MB. 2007. ROS as signalling molecules: mechanisms that generate
518 specificity in ROS homeostasis. Nat Rev Mol Cell Biol 8:813-824.
519 55. Rhee SG. 2006. Cell signaling. H_2O_2, a necessary evil for cell signaling. Science 312:1882-1883.
520 56. Moliere N, Hossmann J, Schafer H, Turgay K. 2016. Role of Hsp100/Clp Protease Complexes in
521 Controlling the Regulation of Motility in *Bacillus subtilis*. Front Microbiol 7:315.

bioRxiv preprint doi: https://doi.org/10.1101/337402; this version posted June 2, 2018. The copyright holder for this preprint (which was not certified by peer review) is the author/funder. All rights reserved. No reuse allowed without permission.

522 57. Shiwa Y, Yoshikawa H, Tanaka T, Ogura M. 2015. *Bacillus subtilis degSU* operon is regulated by
523 the ClpXP-Spx regulated proteolysis system. J Biochem 157:321-330.
524 58. Gerth U, Kruger E, Derre I, Msadek T, Hecker M. 1998. Stress induction of the *Bacillus subtilis*
525 *clpP* gene encoding a homologue of the proteolytic component of the Clp protease and the
526 involvement of ClpP and ClpX in stress tolerance. Mol Microbiol 28:787-802.

527

528

bioRxiv preprint doi: https://doi.org/10.1101/337402; this version posted June 2, 2018. The copyright holder for this preprint (which was not certified by peer review) is the author/funder. All rights reserved. No reuse allowed without permission.

529 **Figure caption**

530 **Fig. 1 The scheme of proline degradation pathway in *B. licheniformis* WX-02. Pro1, γ-glutamyl**
531 **kinase; Pro2, γ -glutamyl phosphate reductase; Pro3, P5C reductase; YcgM, proline oxidase; ycgN,**
532 **P5C dehydrogenase; TCA cycle, the tricarboxylic acid cycle.**

533 **Fig. 2 The γ-PGA yields of *ycgM* and *ycgN* deletion strains (A); complements strains WXΔ*ycgN*-N,**
534 **WXΔ*ycgMN*, WX/*ycgM* and WX/*ycgN* (B).**

535 **Fig. 3 Comparison of γ-PGA synthesie (A), cell growth (B) and glucose consumption (C) of *ycgM***
536 **and *ycgN* deletion strains during γ-PGA production. Values are averages from three biological**
537 **replicates .**

538 **Fig. 4 The intracellular concentrations of proline (A) and P5C (B) in *ycgM* and *ycgN* deletion strains.**
539 **Data represent the mean and standard deviation from three independent experiments. DCW means**
540 **dry cell weight.**

541 **Fig. 5 The intracellular concentrations of ROS in the mutants and its effects on γ-PGA synthesis. The**
542 **intracellular concentrations of ROS in *ycgM*, *ycgN* single mutant and double mutants (A). Effects of**
543 **exogenous antioxidant addition on the level of intracellular ROS (B). Effects of exogenous**
544 **antioxidant addition on γ-PGA synthesis (C). The intracellular ATP concentrations of mutant strains**
545 **during γ-PGA fermentation (D).**

546 **Fig. 6 Effects of *ycgN* delection on the relative transcriptional levels of genes in TCA cycle and γ-PGA**
547 **biosynthesis.**

548 **Fig. 7 The proposed mechanism of the influence of proline metabolism on γ-PGA synthesis. Arrows**
549 **indicate activation or promotion; T bars indicate repression or inhibition. Solid lines indicate**

bioRxiv preprint doi: https://doi.org/10.1101/337402; this version posted June 2, 2018. The copyright holder for this preprint (which was not certified by peer review) is the author/funder. All rights reserved. No reuse allowed without permission.

550 **empirical supports for regulation, and dashed lines indicate supports by inferences where the**

551 **mechanism of regulation is unknown.**

552 **Fig. S1 Effects of H_2O_2 dose on cell growth and γ-PGA production of WX-02.**

553

554

bioRxiv preprint doi: https://doi.org/10.1101/337402; this version posted June 2, 2018. The copyright holder for this preprint (which was not certified by peer review) is the author/funder. All rights reserved. No reuse allowed without permission.

555

Table 1 The strains and plasmids used in this study.

Strains or plasmids	Description	Source
Strains		
B. licheniformis		
WX-02	Polyglutamate productive strain (CCTCC M208065)	Laboratory stock
WXΔ*ycgM*	*B. licheniformis* WX-02 carrying an in-frame deletion in *ycgM* gene	This study
WXΔ*ycgN*	*B. licheniformis* WX-02 carrying an in-frame deletion in *ycgN* gene	This study
WXΔ*ycgMN*	*B. licheniformis* WX-02 carrying an in-frame deletion in *ycgM* and *ycgN* gene	This study
WX/pHY300	WX-02 harboring pHY300PLK	This study
WX/*ycgM*	WX-02 harboring pHY-*ycgM*	This study
WX/*ycgN*	WX-02 harboring pHY-*ycgN*	This study
WXΔ*ycgN*-N	WXΔ*ycgN* complemented with *ycgN* inserted in the genome at *amyL* locus.	This study
Escherichia coli		
DH5α	F^{-} Φ80d/*lac*ZΔM15, Δ(*lacZYA-argF*)U169, *recA*1, *endA*1, *hsdR*17(rK^{-}, mK^{+}),*phoA*, *supE*44, λ^{-}, *thi*-1, *gyrA*96, *relA*1	Laboratory stock
Plasmids		
T2(2)-ori	E. coli-B. licheniformis shuttle vector, OripUC/Orits, Kan	Laboratory stock
T2-*ycgM*	T2(2)-ori derivative, carrying homology arms for the deletion of *ycgM* gene	This study
T2-*ycgN*	T2(2)-ori derivative, carrying homology arms for the deletion of *ycgN* gene	This study
T2-*ycgMN*	T2(2)-ori derivative, carrying homology arms for the deletion of *ycgM* and *ycgN* gene	This study
T2-P_{srf}-*ycgN*	T2(2)-ori derivative, carrying amyl:: (P_{srf}-*ycgN*)	This study
pHY300PLK	*E. coli-B. licheniformis* shuttle vector, Ap^{r}(*E. coli*), Tc^{r}(*E. coli* and *B. licheniformis*)	This study
pHY-*ycgM*	pHY300PLK containing P_{srf} promoter, the gene *ycgM* and *amyL* terminator	This study
pHY-*ycgN*	pHY300PLK containing P_{srf} promoter, the gene *ycgN* and *amyL* terminator	This study

556

557

bioRxiv preprint doi: https://doi.org/10.1101/337402; this version posted June 2, 2018. The copyright holder for this preprint (which was not certified by peer review) is the author/funder. All rights reserved. No reuse allowed without permission.

Table 2 The primers used in this research.

Primers names	**Sequence 5'→3'** [a]
ycgM-A-F	CG**GGATCC**CGTGACGAACTTACGGAAGACGG
ycgM-A-R	CGTCTCATAAAGTATCCGTACCAGCGATTCAGGATGCTGCTTTTAG
ycgM-B-F	CTAAAAGCAGCATCCTGAATCGCTGGTACGGATACTTTATGAGACG
ycgM-B-R	GC**TCTAGA**GCAATAACAACCGTAACACCAGTCG
ycgM-F	GCCCGATTCTGGCTTGC
ycgM-R	TCCACCAAATAATCCCCGAC
ycgN-kA-F	CG**GGATCC**CGTGAAGTGCGCTGCCAAAAG
ycgN-kA-R	GTGAAGCGCAAGATAATCAGGTC TTTTTCGAATGCCTTCCGG
ycgN-kB-F	CCGGAAGGCATTCGAAAAAGACCTGATTATCTTGCGCTTCAC
ycgN-kB-R	GC**TCTAGA**GCCGGAAACCATTCCAGATGATAC
ycgN-F	GCTCAGGAACAGCTTAATTCAC
ycgN-R	GCTTCTCCAGGTCCTCCCG
ycgMN-kA-R	GTGAAGCGCAAGATAATCAGGTCCGATTCAGGATGCTGCTTTTAG
ycgMN-kB-F	CTAAAAGCAGCATCCTGAATCGGACCTGATTATCTTGCGCTTCAC
T2-F	ATGTGATAACTCGGCGTA
T2-R	GCAAGCAGCAGATTACGC
pHY300-F	GTTTATTATCCATACCCTTAC
pHY300-R	CAGATTTCGTGATGCTTGTC
P_{srf}-F	CGGGATCC CGGACGCTCTTCGCAAGGGTGTC
P_{srf}-R	ATTGTCATACCTCCCCTAATC
TamyL-F	AAGAGCAGAGAGGACGGATT
TamyL-R	GCTCTAGA GC CGCGCAATAATGCCGTCGC
ycgM-F:	GGTAAGAGAGGAATGTACACATGAAATGGAAGTGATAACAAGAG ACT
ycgM-R	GAAATCCGTCCTCTCTGCTCTT CCCTTTTTATCGTTTTATTTCTTC
ycgN-F	GATTAGGGGAGGTATGACAA ATGACAACACCTTACAAACACG
ycgN-R	TCCGTCCTCTCTGCTCTT CCCTGTTTAACCCCTTTTCTTAC

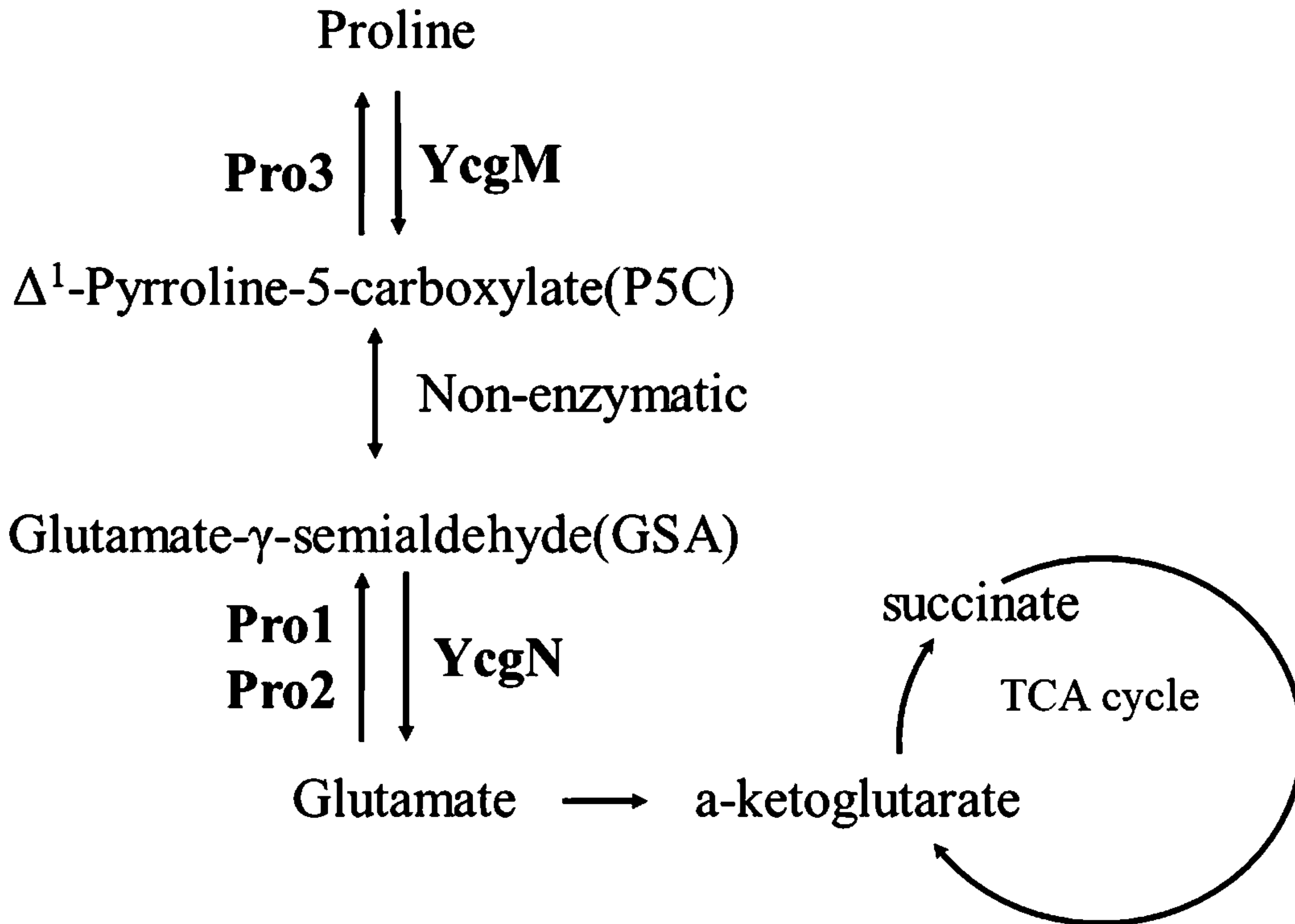
Proline
Pro3
YcgM
Δ1-Pyrroline-5-carboxylate(P5C)
Non-enzymatic
Glutamate-γ-semialdehyde(GSA)
Pro1
Pro2
YcgN
Glutamate
a-ketoglutarate
succinate
TCA cycle

bioRxiv preprint doi: https://doi.org/10.1101/337402; this version posted June 2, 2018. The copyright holder for this preprint (which was not certified by peer review) is the author/funder. All rights reserved. No reuse allowed without permission.

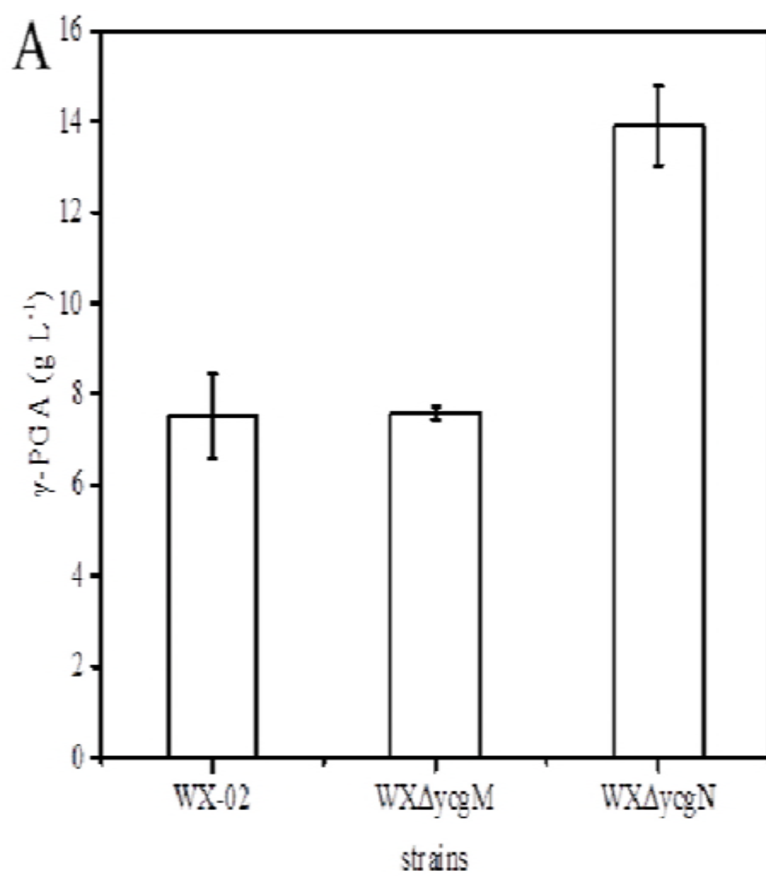

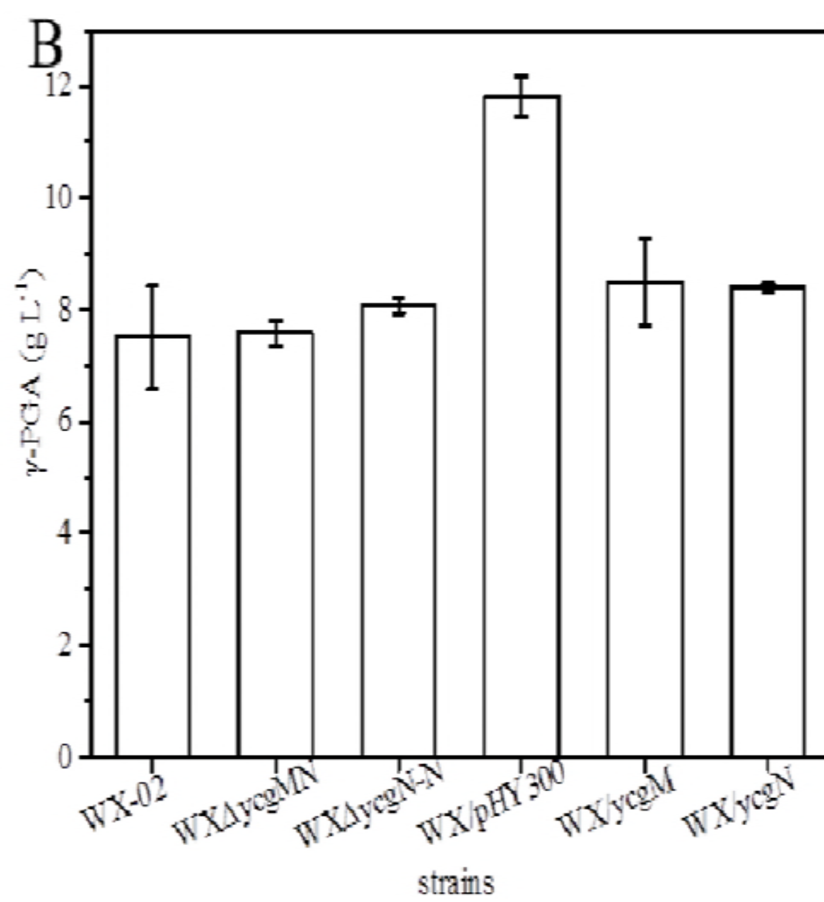

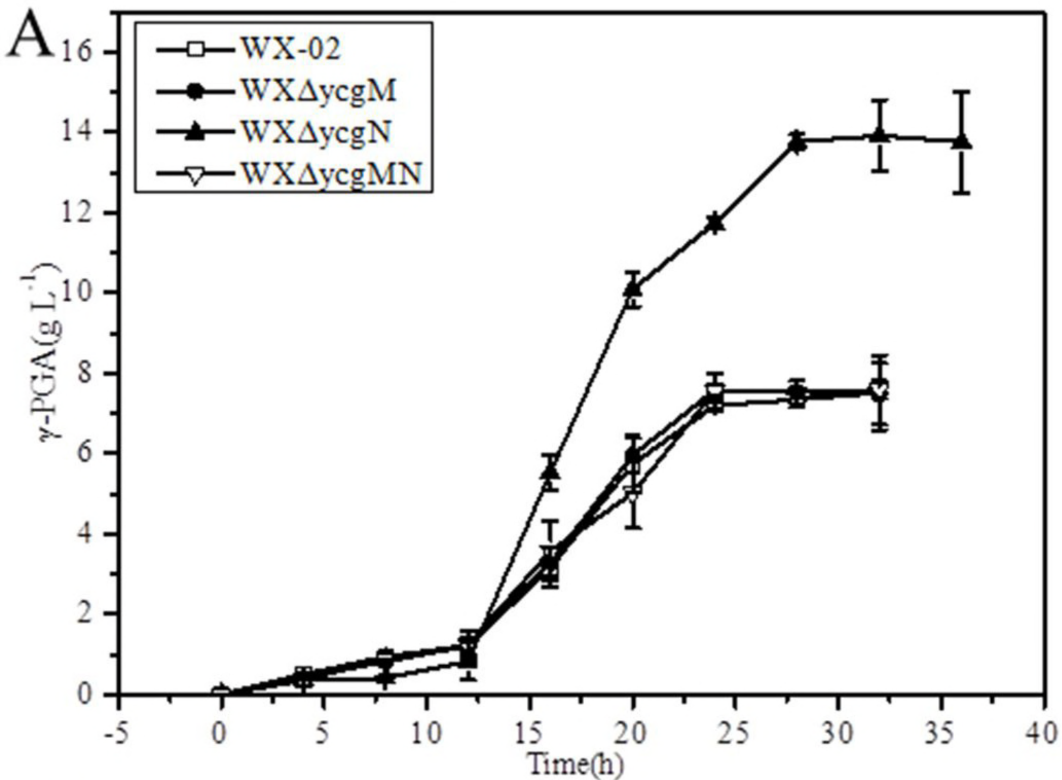
A
WX-02
WXΔycgM
WXΔycgN
WXΔycgMN
γ-PGA(g L-1)
Time(h)
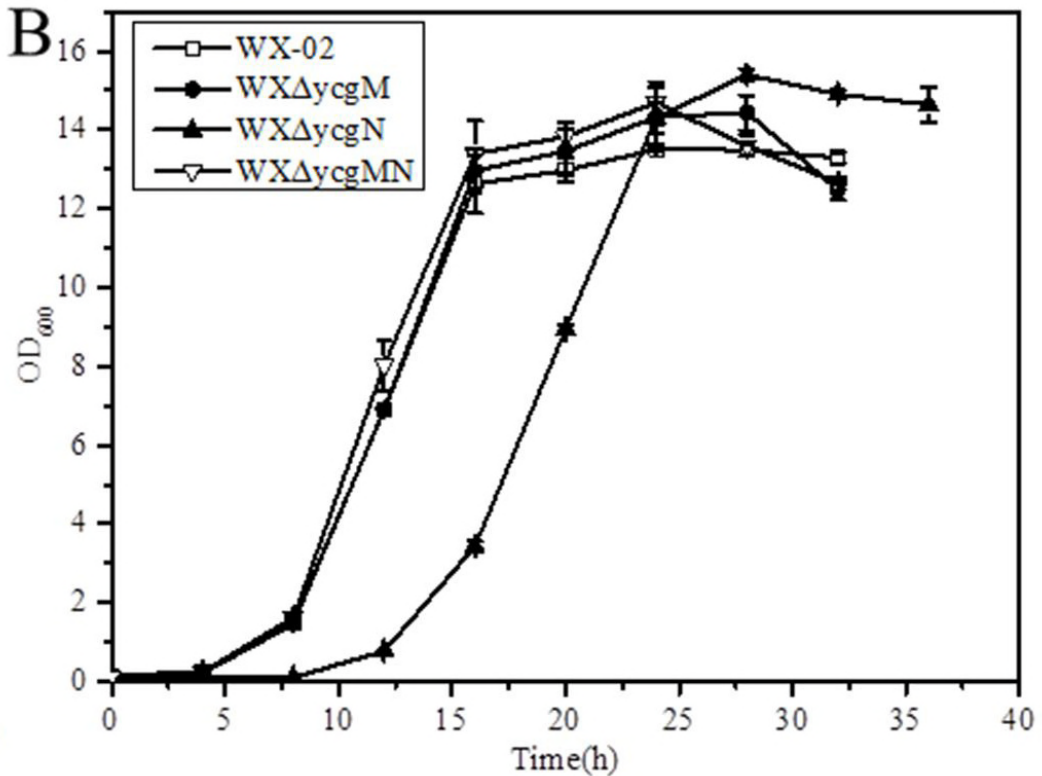
B
WX-02
WXΔycgM
WXΔycgN
WXΔycgMN
OD600
Time(h)
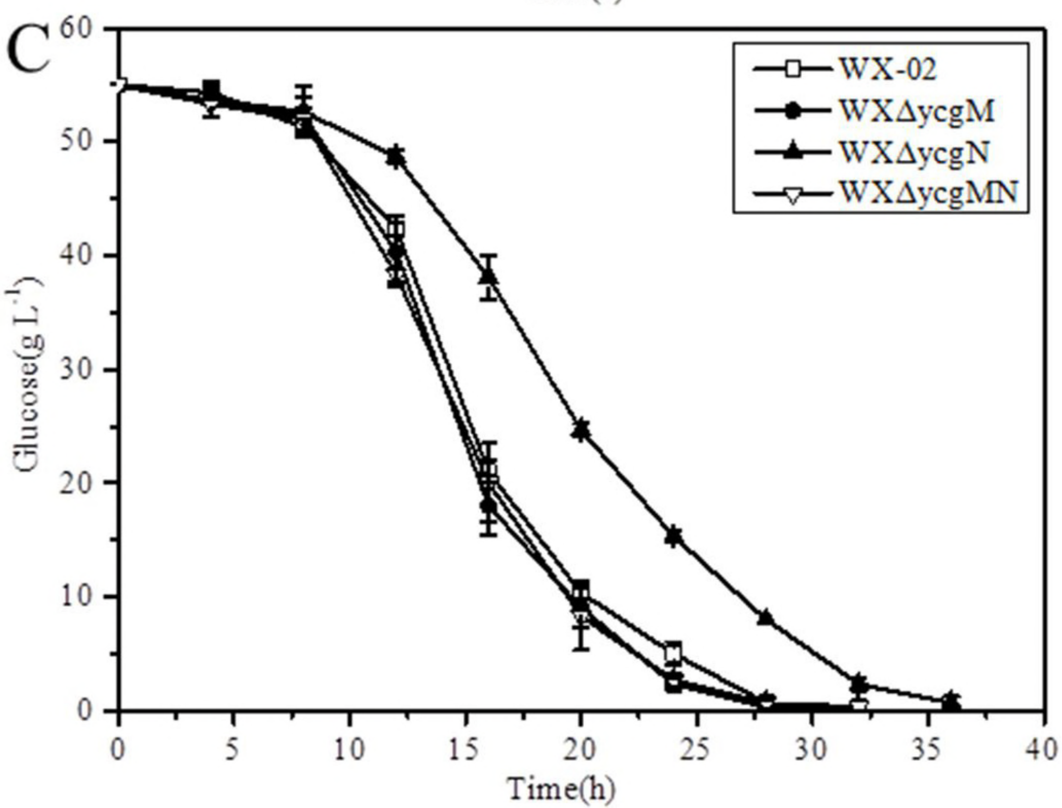
C
WX-02
WXΔycgM
WXΔycgN
WXΔycgMN
Glucose(g L-1)
Time(h)

bioRxiv preprint doi: https://doi.org/10.1101/337402; this version posted June 2, 2018. The copyright holder for this preprint (which was not certified by peer review) is the author/funder. All rights reserved. No reuse allowed without permission.

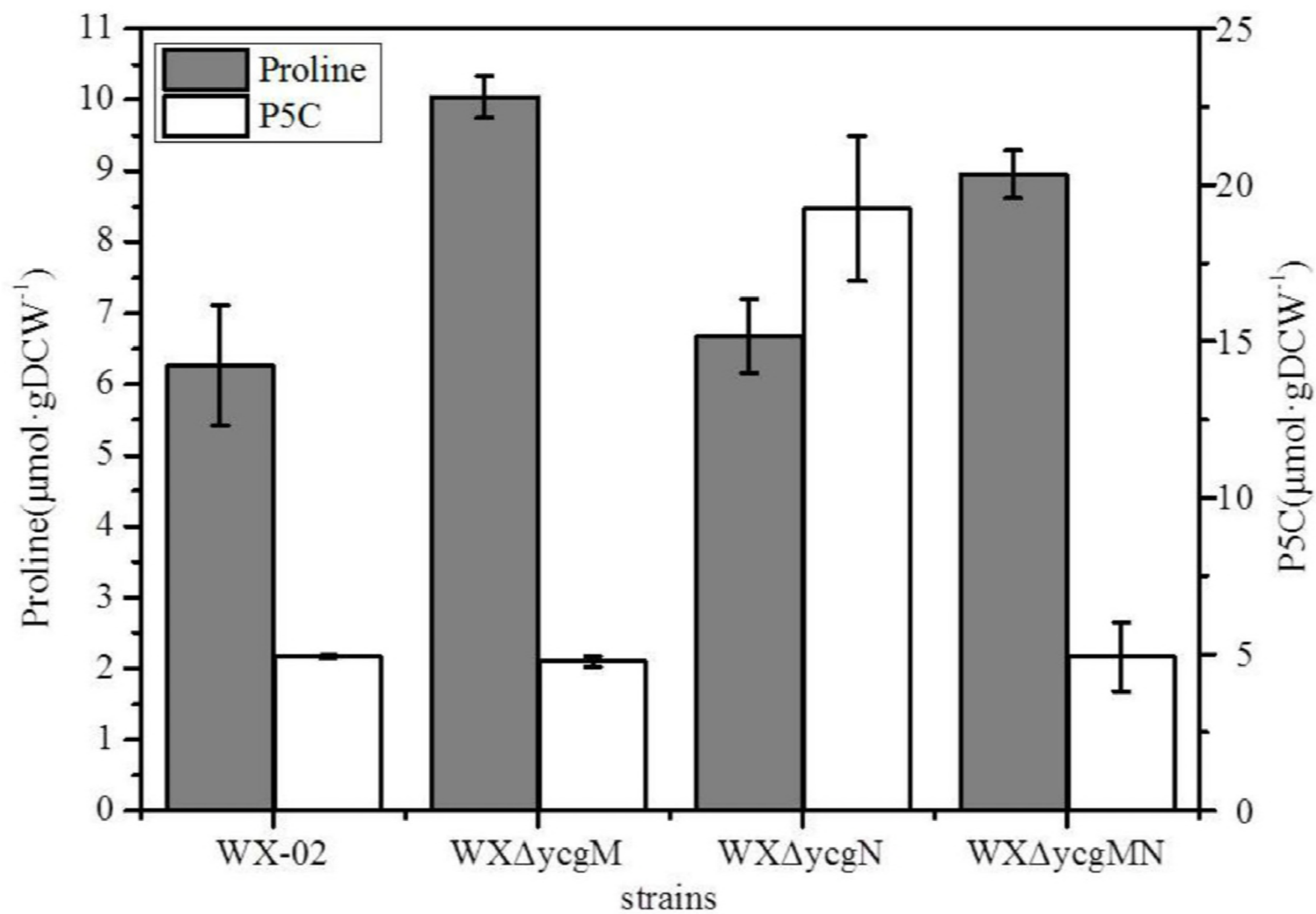

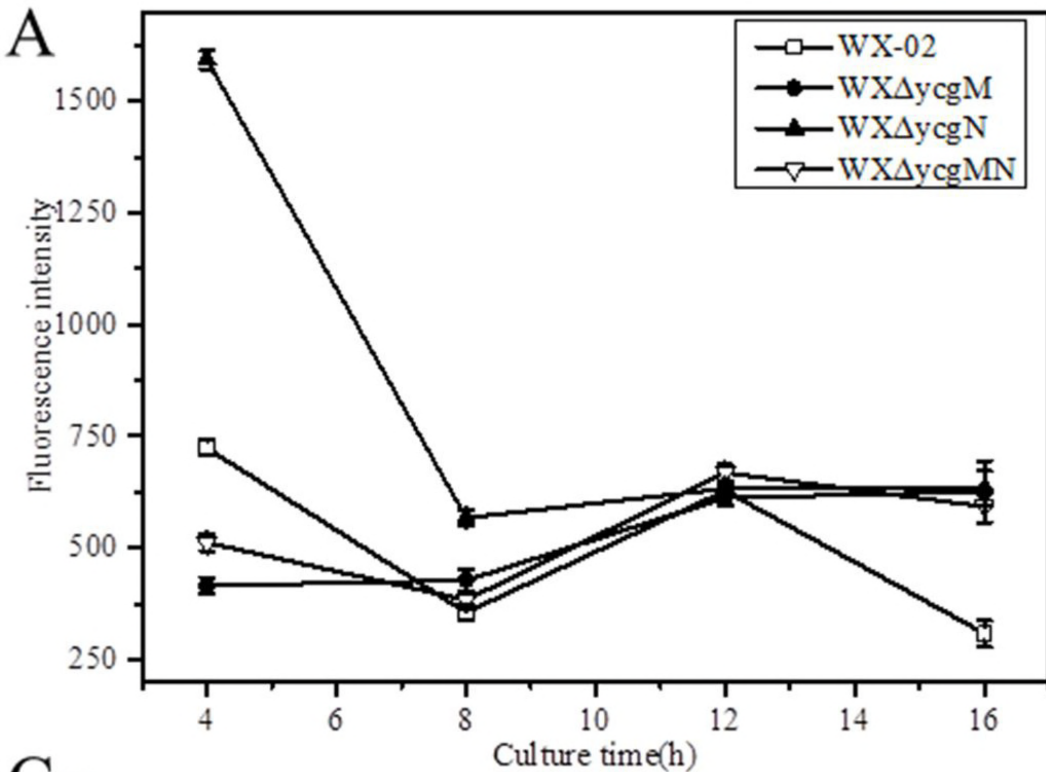
A
WX-02
WXΔycgM
WXΔycgN
WXΔycgMN
Fluorescence intensity
Culture time(h)

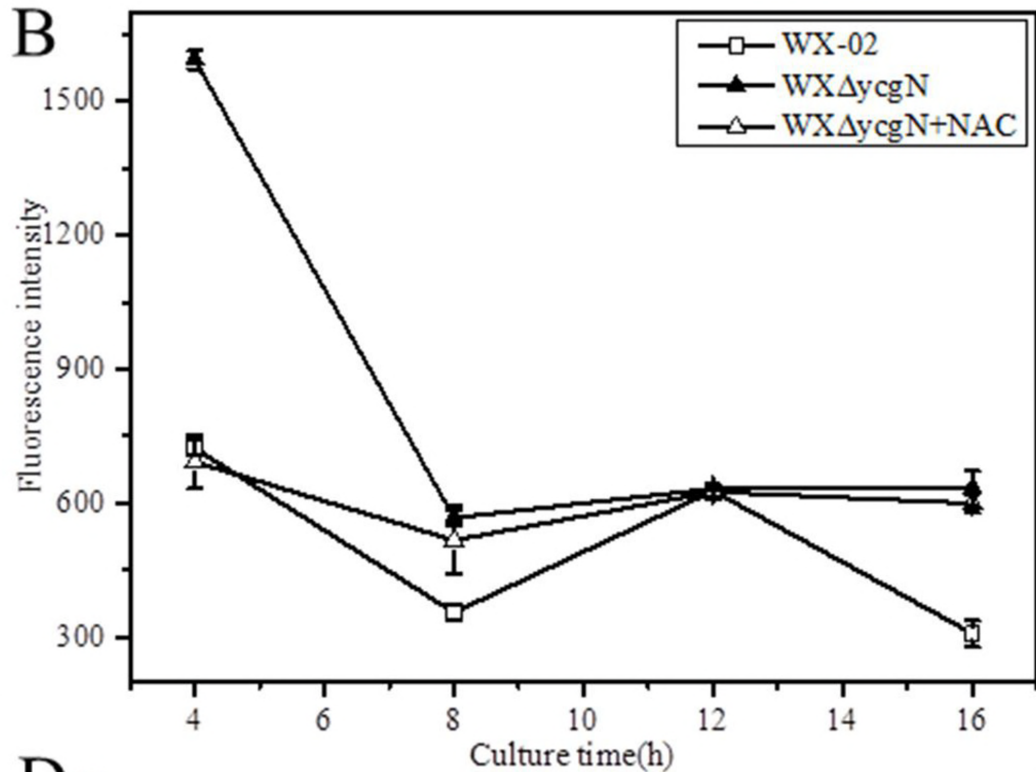
B
WX-02
WXΔycgN
WXΔycgN+NAC
Fluorescence intensity
Culture time(h)

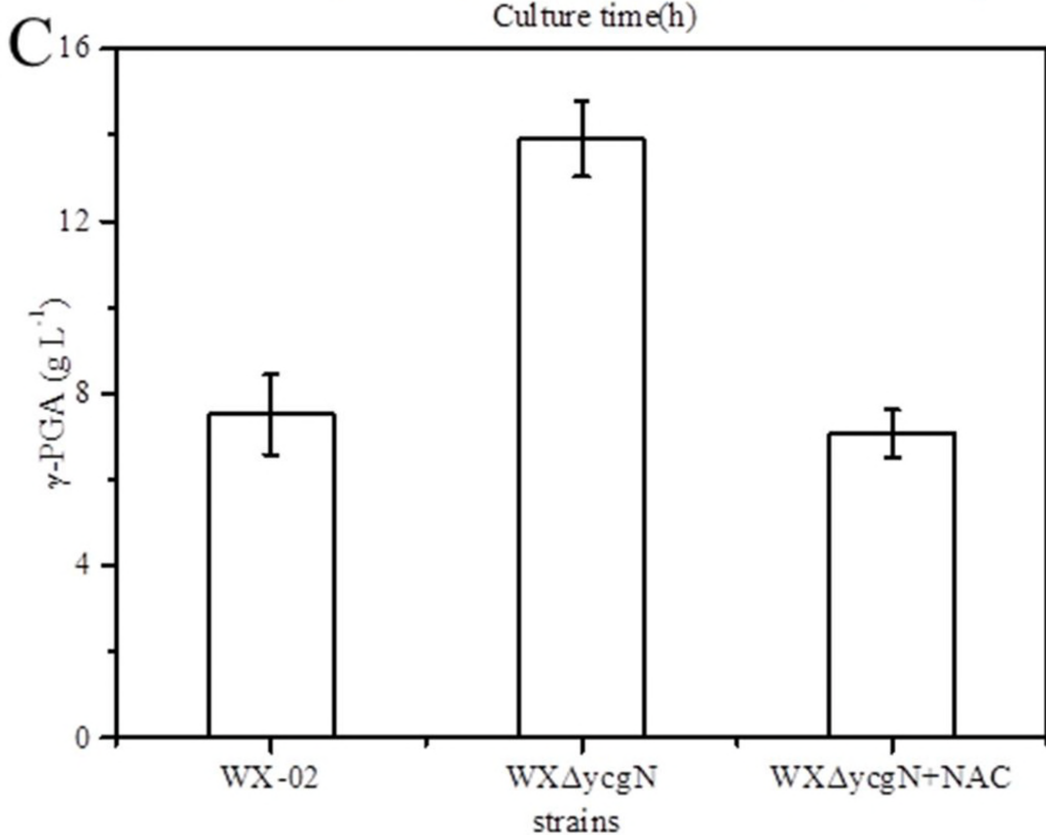
C
γ-PGA (g L-1)
WX-02
WXΔycgN
WXΔycgN+NAC
strains

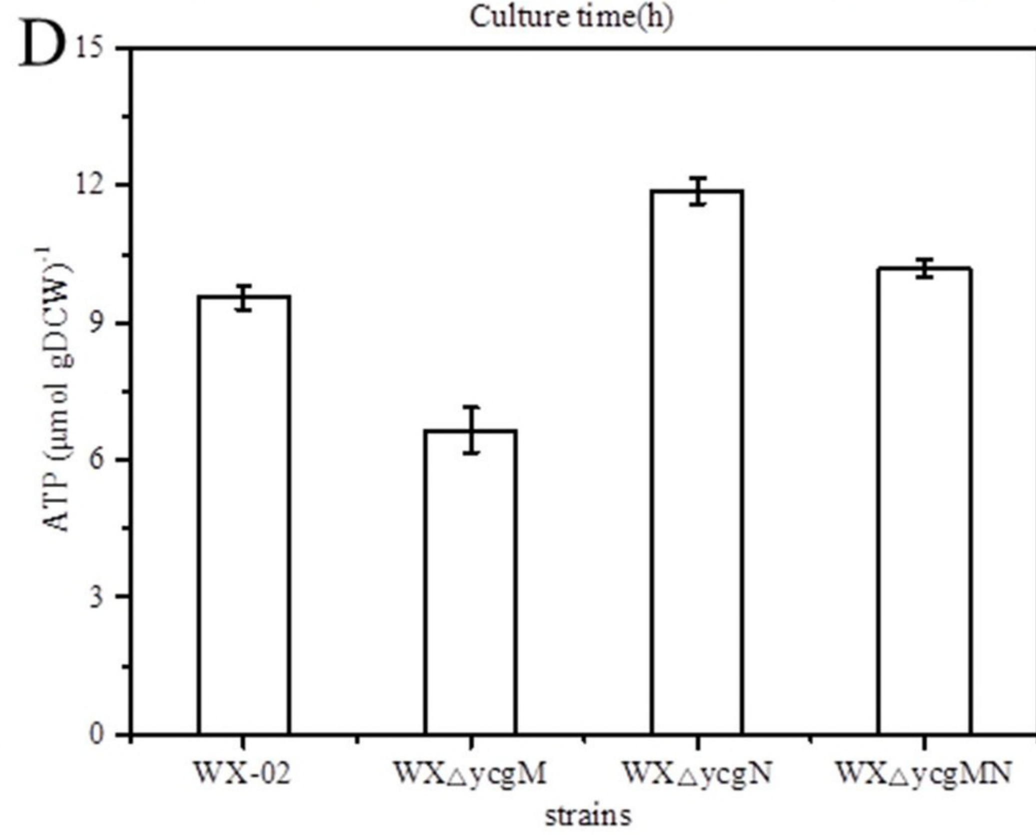
D
ATP (μmol gDCW)-1
WX-02
WX△ycgM
WX△ycgN
WX△ycgMN
strains

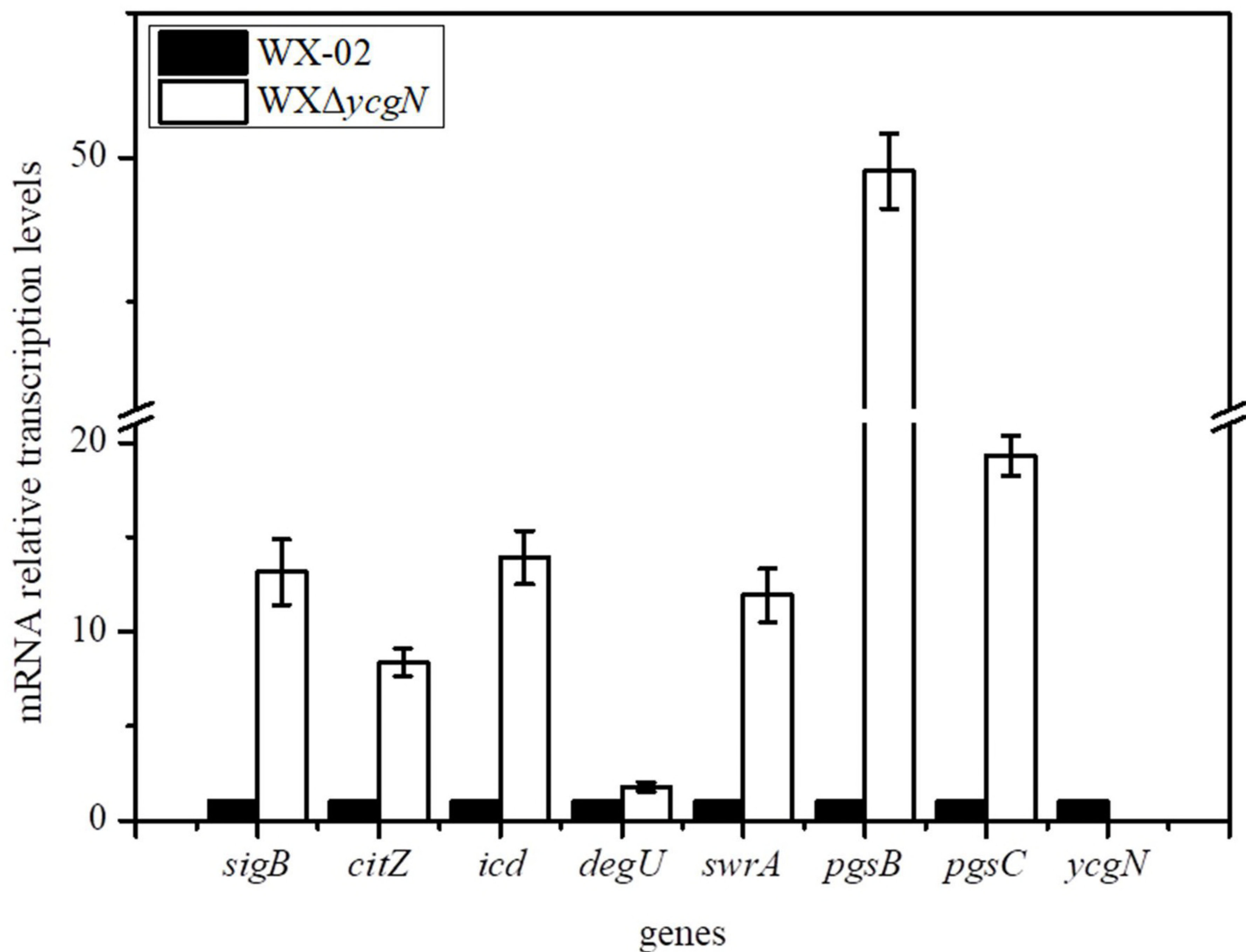
WX-02
WXΔycgN
mRNA relative transcription levels
50
20
10
0
sigB
citZ
icd
degU
swrA
pgsB
pgsC
ycgN
genes

bioRxiv preprint doi: https://doi.org/10.1101/337402; this version posted June 2, 2018. The copyright holder for this preprint (which was not certified by peer review) is the author/funder. All rights reserved. No reuse allowed without permission.